Journal of Chromatography A, 1217 (2010) 990–999

Contents lists available at ScienceDirect

Journal of Chromatography A

journal homepage: www.elsevier.com/locate/chroma

Transition from enantioselective high performance to ultra-high performance liquid chromatography: A case study of a brush-type chiral stationary phase based on sub-5-micron to sub-2-micron silica particles

Giovanna Cancelliere[a], Alessia Ciogli[a], Ilaria D'Acquarica[a], Francesco Gasparrini[a,*], Jelena Kocergin[b], Domenico Misiti[a], Marco Pierini[a], Harald Ritchie[c], Patrizia Simone[a], Claudio Villani[a]

[a] Dipartimento di Chimica e Tecnologie del Farmaco, Sapienza Università di Roma, Piazzale Aldo Moro 5, 00185 Rome, Italy
[b] Regis Technologies, Inc., 8210 Austin Avenue, Morton Grove, IL 60053, USA
[c] Thermo Fisher Scientific, 93-96 Chadwick Road, Runcorn, United Kingdom

ARTICLE INFO

Article history:
Available online 14 October 2009

Keywords:
Chiral stationary phase (CSP)
Enantioselective HPLC
Enantioselective UHPLC
Fast HPLC
Reduced particle size
Sub-2-micron particles

ABSTRACT

Three brush-type chiral stationary phases (CSPs) differing in the particle size of the starting silica particles have been prepared by covalent grafting of the π-acidic bis-(3,5-dinitrobenzoyl)-derivative of *trans*-1,2-diaminocyclohexane (DACH-DNB). Starting silica particles of 4.3, 2.6 and 1.9 micron were used to generate the final CSPs using an improved, highly reproducible synthetic methodology, that allowed to assemble and surface-graft the whole chiral selector in only two steps. The different CSPs have been packed in columns of various length and diameters, and fully characterized in terms of flow permeability, kinetic performances and enantioselectivity using a set of test solutes. Very high speed and high resolution applications together with stereodynamic HPLC examples are demonstrated on the columns with reduced particle diameters, on which separations of several enantiomeric pairs are routinely obtained with analysis times in the 15–40 s range.

© 2009 Elsevier B.V. All rights reserved.

1. Introduction

The ever increasing number of samples to be analyzed in various fields related to the chiral technologies requires improved chromatographic methods that are at the same time fast and robust [1]. Due to its simplicity and versatility, one of the most widely used chromatographic methods to separate and quantitate enantiomers is based on their direct HPLC resolution on chiral stationary phases [2–4]. HPLC columns packed with CSPs are nowadays available in "standard" formats for the column dimensions, with lengths and diameters typically in the 150–250 and 2–4.6 mm range, respectively. Packing materials are also essentially restricted to silica based, 3–5 micron spherical particles.

A substantial increase in the sample throughput of an enantioselective HPLC (e-HPLC) system can be in principle obtained by employing smaller particles packed in short columns and using high linear velocities of the eluent [5–14]. The small particle size approach is now feasible as manufacturers can produce silica based materials with narrow size distributions at the sub-2-micron regime. Several hardware designs together with dedicated particulate materials have been introduced in the last years, together with the corresponding acronyms (UHPLC, ultra-high pressure liquid chromatography; RRLC, rapid resolution liquid chromatography, etc.)

Practical difficulties that one can expect following the sub-2-micron particle approach are twofold: one is inherently related to the decrease of column permeability that accompanies the particle size reduction, the other one is associated to the adaptation of the surface modification chemistry of classical CSPs to smaller particles. The column permeability reduction is linked to the increase in pressure that is proportional to the inverse of the particle diameter squared: thus, reducing the particle diameter by a factor of 3 will result in a ninefold increase in the column back pressure. As a consequence, depending on the column length and eluent viscosity, the full potential of high speed separations can only be exploited on chromatographic hardware that can withstand elevated pressures (UHPLC). An additional complication may arise from the pronounced propensity of the smaller particles to aggregate during synthetic steps leading to a final (chiral) stationary phase with non-optimal performances essentially in terms of permeability and/or efficiency. Mechanical resistance and long term stability of the packed bed are also of major concern when high flow (and hence high pressure) applications are planned.

* Corresponding author.
E-mail address: francesco.gasparrini@uniroma1.it (F. Gasparrini).

0021-9673/$ – see front matter © 2009 Elsevier B.V. All rights reserved.
doi:10.1016/j.chroma.2009.10.021

The aim of this study was to evaluate the use of reduced particle size in combination with an established chiral selector for the generation of advanced brush-type CSPs with high throughput and/or high resolution capabilities. The choice of a brush-type CSP to investigate the potentials of reduced particles in this field was dictated by the excellent kinetic performances of brush-type materials that should constructively combine with those of very small particles (2.0–2.5 micron) and sub-2-micron packings. Our strategy uses an adapted synthetic scheme that is more rugged and reproducible, and yields CSPs that are consistent in terms of surface coverage, chemio- and enantioselectivity. The columns packed with CSPs based on 2.6 and 1.9 micron particles show enhanced kinetic performances compared to those packed with 4.3 micron particles, allowing for sub-minute enantioseparations in the UHPLC regime (e-UHPLC).

2. Experimental

2.1. Materials and methods

HPLC gradient grade dichloromethane, hexane, chloroform stabilized with ethanol, 1,4-dioxane and methanol were obtained from Carlo Erba Reagents (Rodano, MI, Italy); HPLC grade 2-propanol was purchased from Sigma–Aldrich (Milano, Italy). (*S,S*)-Diaminocyclohexane (DACH), glycidoxypropyltrimethoxysilane (GOPTMS), 3,5-dinitrobenzoylchloride (3,5-DNB-Cl), diisopropylethylamine (DIPEA), triethylamine (TEA), 1-(trimethylsilyl)-imidazole, tri-*tert*-butyl benzene and solvents used for reactions were all of analytical grade and originated from Sigma–Aldrich (Milano, Italy). Spherical Daisogel SP-120-5P (pore size 127 Å, particle size 4.3 μm and specific surface area 306 $m^2 g^{-1}$) and SP-120-2.5P (pore size 125 Å, particle size 2.6 μm and specific surface area 343 $m^2 g^{-1}$) silica gels were a gift from Daiso Chemical (Osaka, Japan), spherical Hypurity Thermo (pore size 190 Å, particle size 1.9 μm and specific surface area 200 $m^2 g^{-1}$) silica was a gift from Thermo Scientific (Waltham, MA, USA).

2.2. Preparation of the DACH-DNB chiral stationary phases (DACH-DNB-CSPs)

All reactions were carried out in a lab-modified Rotavapor-M rotary evaporator (Büchi, Flawil, Switzerland), in which the reaction flask was fitted with solvent condenser, solvent collector, argon inlet and allowed syringe addition of reactant solutions and isolation of the solid materials by filtration under an inert atmosphere. Mixing was obtained by spinning the flask around its axis.

Step 1 (DACH-CSP)—a slurry of 3.5 g of silica gel and 2.4 g of (*S,S*)-diaminocyclohexane ($C_6H_{14}N_2$, Mw 114.19, 20.7 mmole) in MeOH (12 ml) was heated to reflux under argon atmosphere and continuous stirring. A solution of glycidoxypropyltrimethoxysilane ($C_9H_{20}SiO_5$, Mw 236.34, 2.3 mmole, *d*: 1.07 g/ml) in MeOH (0.5 ml in 10 ml) was added dropwise during 1 h. The mixture was heated to reflux for ~8 h. After cooling to r.t., modified silica gel was isolated by filtration, washed with MeOH, CH_2Cl_2 (50 ml each) and dried *in vacuo* (0.1 mmHg) at *T* = 50 °C to constant weight.

FT-IR (KBr): 2938, 2862, 1878, 1622, 1456, 1088 cm^{-1}. Elemental analysis: C 6.93%, H 1.39%, N 1.19% for 4.3 μm silica gel; C 6.83%, H 1.42%, N 1.09% for 2.6 μm silica gel and C 3.44%, H 0.74%, N 0.61% for 1.9 μm silica gel.

Step 2 (DACH-DNB-CSP)—a slurry of DACH-CSP (4.0 g) and 2 ml of diisopropylethylamine ($C_8H_{19}N$, Mw 129.25, 11.6 mmole, *d*: 0.75 g/ml) in dry THF (40 ml) was cooled at 0 °C in an ice bath. Under argon atmosphere and continuous stirring, a solution of 3.5 g of 3,5-dinitrobenzoylchloride ($C_7H_3ClN_2O_5$, Mw 230.56, 15.2 mmole) in dry THF (13 ml) was added dropwise, then the ice bath was removed and the mixture was heated to reflux for 3.5 h. After cooling to r.t., modified silica gel was collected by filtration, washed with THF, MeOH, H_2O, acetone, CH_2Cl_2 (50 ml each) and dried *in vacuo* (0.1 mmHg) at *T* = 50 °C to constant weight. FT-IR (KBr): 2948, 2280, 1549, 1346, 1086 cm^{-1}. Elemental analysis: C 10.02%, H 1.45%, N 2.18% for 4.3 μm silica gel; C 10.36%, H 1.36%, N 2.18% for 2.6 μm silica gel and C 5.83%, H 0.79%, N 1.31% for 1.9 μm silica gel.

Step 3 (*End capping*)—3.5 g of DACH-DNB-CSP was added to a solution of 1-(trimethylsilyl)-imidazole (1.70 ml, $C_6H_{12}N_2Si$, Mw 140.26, 11.6 mmole, *d*: 0.96 g/ml) in dry toluene (30 ml). The mixture was mechanically stirred and heated to reflux for 4 h. After cooling to r.t., end-capped silica was isolated by filtration, washed with toluene, MeOH, MeOH/TEA 99/1, MeOH, CH_2Cl_2 and dried *in vacuo* (0.1 mmHg) at *T* = 50 °C to constant weight. Final elemental analysis: C 12.93%, H 1.95%, N 2.09% for 4.3 μm silica gel; C 13.13%, H 2.02%, N 2.10% for 2.6 μm silica gel and C 7.47%, H 1.07%, N 1.31% for 1.9 μm silica gel. Elemental analysis data are presented in Table 1.

2.3. Chromatographic set-up

Two different arrangements were optimized for chromatographic runs: UHPLC and HPLC systems. The Acquity® UPLC consisted of a binary solvent manager, sample manager, a "home-made temperature controller" column compartment and PDA [200–400 nm] detector with a 500 nl flow cell (Waters, Milford, MA, USA). The PDA was set with filter time constant of 0.05 s and a sampling rate of 80 points/s. Additionally, for high flow rates (>2 ml/min) and with ~400 bar upper pressure limit, a M510 model pump and a VICI 5 μl loop microelectric valve actuator, operating at up to 1380 bar (Valco® Instruments Co. Inc., Houston, TX, USA) were employed. The HPLC system consisted of a W1525 pump, a "home-made temperature controller" column compartment, a 5 μl loop Rheodyne (Cotati, CA, USA) manual injector and a dual wavelength W2487 UV detector with a 10 μl flow cell (Waters, Milford, MA, USA). To reduce the extracolumn volumes, connecting tubes of 0.1 mm I.D. for UHPLC arrangement and standard tubes of 0.25 mm I.D. for HPLC system were employed.

Data acquisition and processing were performed with the Empower 2 software from Waters (Milford, MA, USA).

2.3.1. Column geometries

Stainless steel columns with different lengths (*L* = 50, 75, 100, 150, 250 mm) and 4.1 mm I.D. were packed with the DACH-DNB-CSP 4.3 μm (**CSP-1**), DACH-DNB-CSP 2.6 μm (**CSP-2**) and DACH-DNB-CSP 1.9 μm (**CSP-3**) using a non-optimized slurry packing procedure. A column with 3.2 I.D. was also prepared using the 2.6 μm CSP. For the column packed with 2.6 and 1.9 μm CSPs, 1 micron end frits were used. Packing pressures were 700 bar for the

Table 1
Physico-chemical data for starting silicas and final DACH-DNB CSPs.

Starting silica	d_p (μm)	Pores (Å)	Surface area (m^2/g)	Elemental analysis of DACH-DNB-CSPs		
				%C	%H	%N
Daisogel SP-120-5P	4.3	127	306	12.93	1.95	2.09
Daisogel SP-120-2.5P	2.6	125	343	13.13	2.02	2.10
Hypurity	1.9	190	200	7.47	1.07	1.31

Table 2
Kinetic and backpressure data for columns (I.D. 4.1 mm) packed with the three DACH-DNB-CSPs using hexane/$CHCl_3$ (90/10) as an eluent at T = 25 °C.

d_p (μm)	L (mm)	$L/d_p \times 10^{-3}$			N_{column}			$t_{0,c}$ (min)	Φ_{opt} (ml/min)	ΔP (bar)
		50–60	30–40	19–25						
4.3	250	58	–	–	23,800			2.605	0.90	37
	150	–	35	–		14,250		1.563		22
	100	–	–	23			9500	1.042		15
2.6	150	58	–	–	22,400			0.894	1.50	94
	100	–	38	–		15,100		0.596		62
	75	–	29	–		11,300		0.447		47
	50	–	–	19			7550	0.298		31
1.9	100	53	–	–	19,300			0.420	2.20	193
	75	–	39	–		14,500		0.315		145
	50	–	26	–			10,000	0.210		96

4.3 μm CSP, 800 bar for the 2.6 μm CSP, and 900 bar for the 1.9 μm CSP. Geometries of the packed columns and the corresponding corrected void times ($t_{0,c}$) are listed in Table 2.

2.3.2. Efficiency test: van Deemter analysis

Column efficiencies were evaluated by injecting a mixture of achiral compounds (benzene, nitrobenzene, acetophenone, methyl benzoate and 1,3-dinitrobenzene) using hexane/$CHCl_3$ 90:10 (v/v) as an eluent, at variable flow rates ranging from 0.2 to 4.0 ml/min at 25 °C, and UV detection at 254 nm. The column hold-up times (t_0) were determined from the elution time of an unretained marker (tri-*tert*-butyl benzene) using CH_2Cl_2/MeOH (97/3) as an eluent, at a flow rate of 1.00 ml/min at 25 °C, and UV detection at 254 nm. The number of theoretical plates was calculated by built-in functions in the Empower software (Waters) using 50% peak width. Eluent linear velocities are calculated from the $\mu_0 = L/t_0$ equation [15], where L is the column length and t_0 is the elution time of a non-retained marker. Resolution values were calculated by built-in functions in the Empower software using the equation $(t_2 - t_1) \times 1.18/(w_2 + w_1)$ where t_2 and t_1 are retention times and w_2 and w_1 are peak widths at 50% of peak height.

All reported column pressure drop, column permeability and retention data were obtained after correction for the system pressure drop and t_0—time measured by replacing the column with a zero dead volume connector.

3. Results and discussion

3.1. Preparation of the chiral stationary phases

We used an improved procedure (Fig. 1) to generate the known DACH-DNB-CSPs [16–19] starting from spherical silica particles with diameters of 4.3, 2.6 and 1.9 micron. The new strategy generates the intermediate DACH-CSP in a single step starting from a slurry of bare silica and the chiral diamine, to which glycidoxypropyltrimethoxysilane is added dropwise. Nucleophilic ring opening of the oxirane by one of the diamine nitrogen atoms is followed by organosilylation of the silica surface, leading to the intermediate material in which the chiral diamine is covalently linked to the silica surface through a flexible spacer. This step is highly reproducible, giving constant results in terms of carbon and nitrogen loadings, and can be easily scaled up to multigram levels. Excess diamine used in this step can be easily recovered by solvent removal and distillation. Final treatment of the intermediate silica with dinitrobenzoyl chloride in the presence of diisopropylethylamine introduces the π-acidic aromatic fragments on the diamine framework through amide linkages. End capping of residual silanols is obtained by treating the stationary phases with 1-(trimethylsilyl)-imidazole. Table 1 summarizes some physical parameters of the starting silicas and the elemental analysis results for the final CSPs. Daisogel SP-120-5P and SP-120-2.5P starting silicas have nearly the same specific surface area (306 and 343 m^2/g, respectively) and give very similar values of carbon and nitrogen contents, for both the intermediate and final silica (see Section 2 and Table 1). Hypurity silica has lower surface area (200 m^2/g) and,

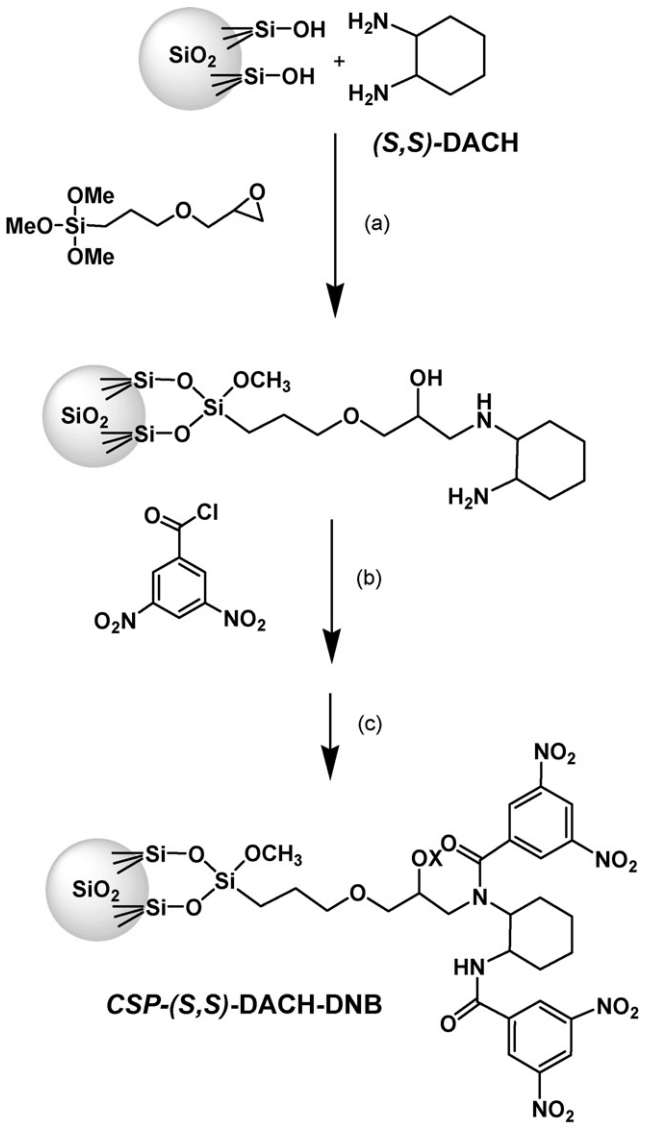

Fig. 1. Synthetic pathway to DACH-DNB CSPs. (a) GOPTMS, MeOH, reflux, 7.5 h; (b) THF, T = 0 °C (addition) then reflux, 4 h; (c) trimethylsilyl-imidazole, toluene reflux, 4 h (X = H or DNB).

Table 3
Retention (k_i) and selectivity ($\alpha_{i,j} = k_i/k_j$) data for achiral test solutes collected on the three DACH-DNB-CSPs using hexane/$CHCl_3$ 90/10 as an eluent at $T = 25\,^{\circ}C$.

Column		Peak 1	Peak 2		Peak 3		Peak 4		Peak 5	
d_p (μm)	V_0 (ml)	k_1	k_2	$\alpha_{2,1}$	k_3	$\alpha_{3,2}$	k_4	$\alpha_{4,3}$	k_5	$\alpha_{5,4}$
1.9	0.911	0.15	0.65	4.33	1.29	1.98	1.87	1.45	3.30	1.76
2.6	0.882	0.26	0.87	3.35	1.54	1.77	1.98	1.29	3.98	2.01
4.3	0.917	0.14	0.66	4.71	1.28	1.94	1.72	1.34	3.25	1.89

Table 4
Kinetic data for columns packed with the three DACH-DNB-CSPs.

Column, d_p (μm)	H_{min} (μm)	h	μ_{opt} (mm/s)	N/m	K_F (10^{-14} m^2)	Speed factor, Sf μ_{opt}	C, Van Deemter term (ms)
4.3	10.5	2.4	1.65	95,238	4.75	1.00	1.43
2.6	6.7	2.6	3.11	149,250	1.27	1.88	0.76
1.9	5.2	2.8	4.00	192,308	0.60	2.42	0.18

Eluent: hexane/$CHCl_3$ 90/10. Solute: methyl benzoate. See text for experimental conditions.

Table 5
Speed factors calculated for columns with different L/d_p ratios. Shaded cells indicate columns studied in the present work.

L (mm)	d_p					
	4.3 μm (μ_{opt} = 1.65 mm/s)		2.6 μm (μ_{opt} = 3.11 mm/s)		1.9 μm (μ_{opt} = 4.00 mm/s)	
	$L/d_p \times 10^{-3}$	Speed	$L/d_p \times 10^{-3}$	Speed	$L/d_p \times 10^{-3}$	Speed
250	58	1.0	96	1.9	132	2.4
150	35	1.7	58	3.2	79	4.1
100	23	2.5	38	4.7_5	53	6.0
75	17	3.3	29	6.3	39	7.9
50	12	5.0	19	9.5	26	12.0

as expected, shows lower carbon and nitrogen loadings in the two reaction steps compared to Daisogel materials.

3.2. Column evaluation: achiral test solutes and flow-pressure plots

The three CSPs have been packed, using a known procedure, at 700 (4.3 μm CSP), 800 (2.6 μm CSP) and 900 (1.9 μm particles) bar into stainless steel columns of various length and inner diameters (see later). For the purpose of characterizing the retention properties (thermodynamics) and the kinetic performances of columns packed with different particle size CSPs, we choose a set of achiral aromatic compounds to monitor retention, selectivity and efficiency (N) under identical conditions. Table 3 gathers the results collected on 100 × 4.1 mm columns packed with the different CSPs using hexane containing 10% of chloroform as an eluent. Clearly, the three CSPs show similar retention behaviors, although retention of the achiral analytes on the CSP based on 2.6 micron is slightly larger than that observed on the other two CSPs, a finding consistent with the higher surface area of the 2.6 micron starting silica. The same eluent mixture consisting of 10% chloroform in hexane was used to evaluate the flow-pressure properties of the three different columns, by monitoring the corrected back pressure values at flow rates ranging from 0.2 to 6.0 ml/min (Fig. 2). Experimental points lie on straight lines for the three columns, with the slope of the lines increasing as the particle size is reduced. The

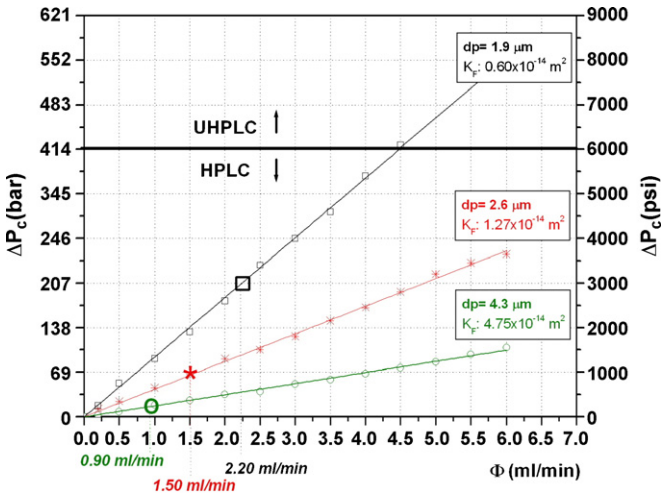

Fig. 2. Flow-pressure plots for the three DACH-DNB CSPs packed on 100 × 4.1 mm columns, using hexane/$CHCl_3$ 90/10 as an eluent at column temperature $T_{col} = 25\,^{\circ}C$.

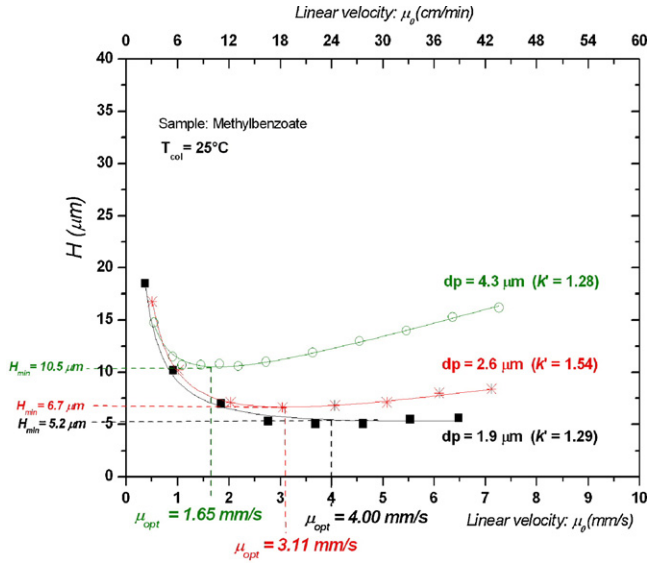

Fig. 3. van Deemter plots for the three DACH-DNB CSPs packed on 100 × 4.1 mm columns, using hexane/$CHCl_3$ 90/10 as an eluent at column temperature $T_{col} = 25\,^{\circ}C$, and methyl benzoate as a test solute.

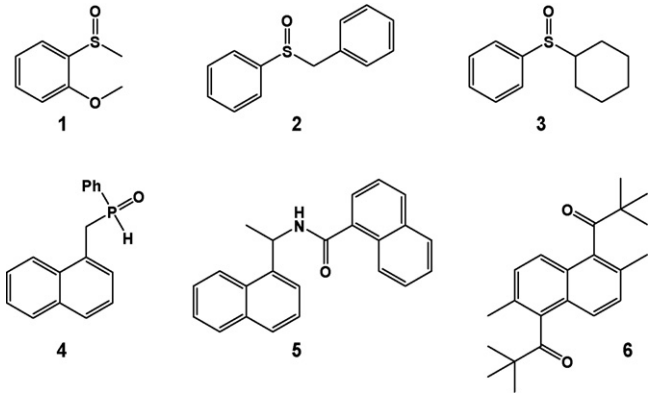

Fig. 4. Structures of the chiral test compounds used to monitor enantioselective separations on DACH-DNB CSPs.

last experimental point collected on the 1.9 μm CSP at high flow rates reaches the UHPLC region of the plot, where column backpressure values exceed 400 bar (~6000 psi). Given the low viscosity of the eluent used (0.43 mPa × s at 25 °C [20]), the high backpressure values observed on the 1.9 μm are never reached with the 2.6 or 4.3 μm CSPs within the eluent flow rates range we have explored. Values of the specific permeability K_F are calculated for the three columns using Eq. (1):

$$K_F = \frac{\eta L \phi}{r^2 \pi \Delta P_c}, \quad (1)$$

where the eluent viscosity, η, is in mPa × s, the length, L, and radius, r, of columns are in mm, the flow rate, ϕ, in ml/min and the corrected column pressure, ΔP_c, is in Pa [21]. The specific permeability values $K_F \times 10^{-14}$ are 0.60, 1.27 and 4.75 m^2 for the 1.9, 2.6 and 4.3 μm CSPs, respectively, using η = 0.43 mPa × s at 25 °C. Fig. 2 also shows the flow rates corresponding to the minima of the van Deemter plots generated using the same eluent and the set of aromatic test solutes (see later): when the three columns are operated at these "optimum" flow rates, the column back pressure observed for the 1.9 μm CSP is three and five times higher than those observed on the 2.6 and 4.3 μm CSPs, respectively.

3.3. Column evaluation: van Deemter analysis

The same chromatographic system comprising the three 100 × 4.1 mm columns packed with 4.3, 2.6 and 1.9 mm DACH-DNB-CSPs, 10% chloroform in hexane as an eluent and the aromatic test solutes, was used to investigate the chromatographic efficiency (number of theoretical plates N and the related height of the theoretical plate H) and its dependence on the eluent flow rate. Given the low viscosity of the organic eluent, we were able to explore an extended range of flow rates, spanning from 0.25 to 6.0 ml/min, corresponding to linear velocities ranging from 0.5 to 7.5 mm/s. The van Deemter curves for the three columns are illustrated in Fig. 3. The minima of the van Deemter curves are H_{min} = 10.5, 6.7 and 5.2 μm for the columns packed with 4.3, 2.6 and 1.9 mm DACH-DNB-CSPs, respectively. The values of the reduced plate height ($h = H/d_p$) for the columns packed with 4.3 and 2.6 μm CSPs are 2.4 and 2.6, respectively, close to the minimum h = 2.0 usually observed

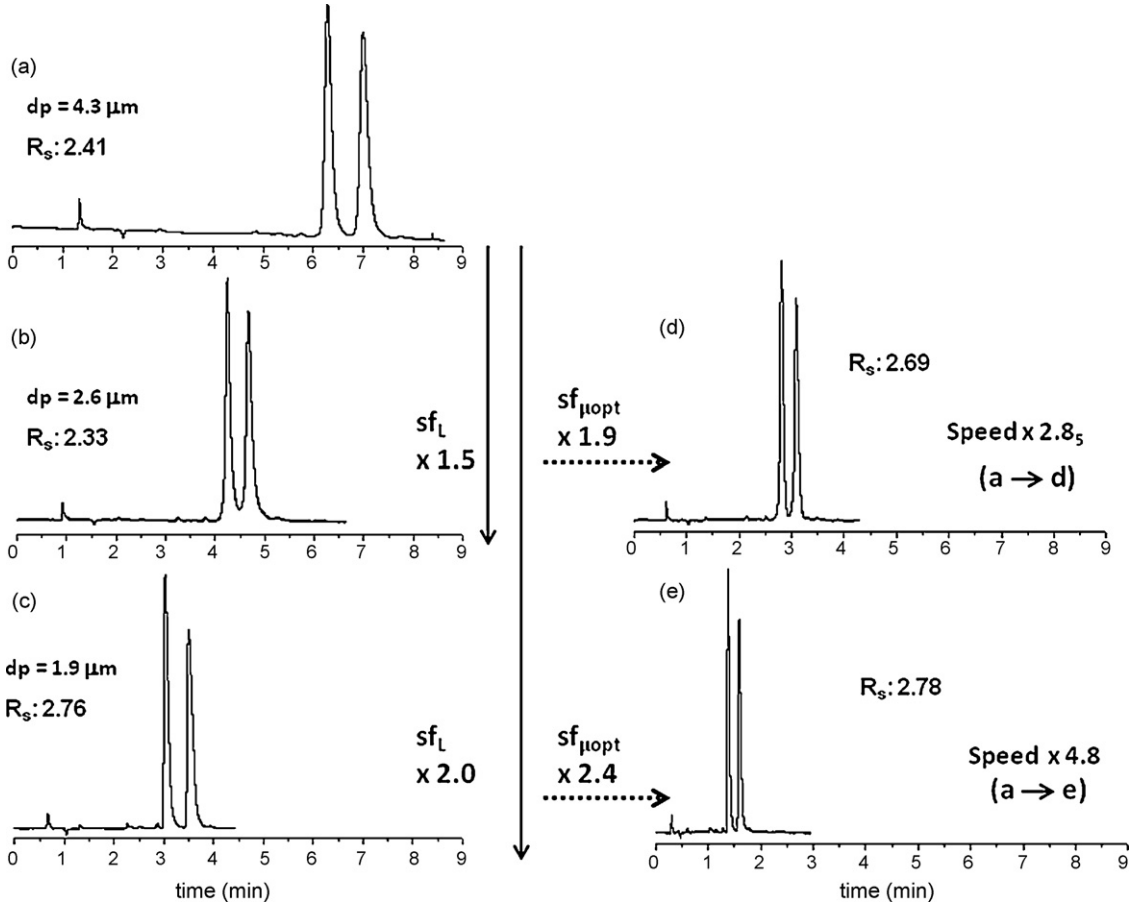

Fig. 5. Resolution of the enantiomers of sulfoxide **1** on the three DACH-DNB CSPs at constant L/d_p ratios and flow rate (a–c) and at the optimum flow rate (d–e). Column dimensions (mm), $L/d_p \times 10^{-3}$ ratios, flow rates (ml/min): (a) 150 × 4.1, 35, 1.00; (b) 100 × 4.1, 38, 1.00; (c) 75 × 4.1, 39, 1.00; (d) 100 × 4.1, 38, 1.50; (e) 75 × 4.1, 39, 2.20. Experimental conditions as in Table 6.

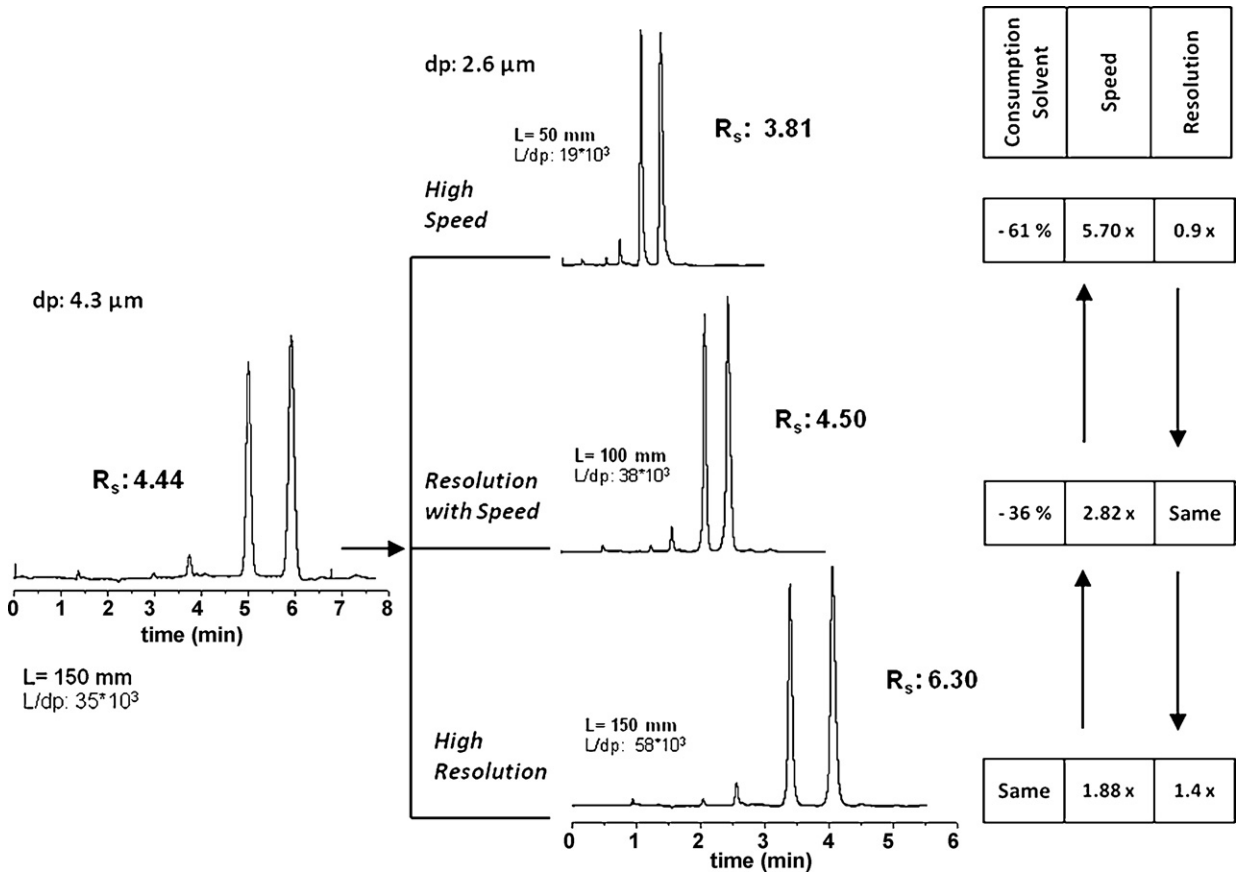

Fig. 6. Resolution of the enantiomers of sulfoxide **2** on DACH-DNB CSPs at different L/d_p ratios and flow rates. Flow rates are 1.00 ml/min (left) and 1.50 ml/min (right). Experimental conditions as in Table 6.

with very well packed columns, whereas the higher value (h = 2.8) observed for the column prepared with 1.9 µm CSP reflects in part a more difficult packing process, that could be improved using specific, optimized packing procedures based also on higher packing pressures.

When the reduced parameters h and ν are used, Eqs. (2)–(5) can be written as

$$N = \frac{L}{d_p} \times \frac{1}{h} \quad (2)$$

$$\nu = \frac{\mu \times d_p}{D_m} \quad (3)$$

$$N_{max} = \frac{L}{d_p} \times \frac{1}{h_{min}} \quad (4)$$

Table 6
Retention and enantioselectivity data for chiral compounds **1**–**5** collected on the three DACH-DNB-CSPs at T = 25 °C.

Compound	CSP, d_p (µm)					
	4.3		2.6		1.9	
	k_1	α	k_1	α	k_1	α
1	3.56[a]	1.15	3.74[a]	1.15	3.40[a]	1.20
2	2.62[a]	1.26	2.70[a]	1.22	2.07[a]	1.40
3	1.82[a]	1.07	2.04[a]	1.20	1.55[a]	1.10
4	1.58[b]	1.78	1.94[b]	1.60	1.32[b]	1.84
5	0.48[c]	2.40	0.68[c]	1.97	0.32[c]	2.97

[a] Eluent: hexane/1,4-dioxane (70/30) + 3%MeOH.
[b] Eluent: hexane/CH_2Cl_2/1,4-dioxane (30/30/40) + 5%MeOH.
[c] Eluent: CH_2Cl_2/IPA (97/3).

$$\nu_{opt} = \mu_{opt} \times \frac{d_p}{D_m} \quad (5)$$

where N_{max} and h_{min} are the values obtained at the minima of the van Deemter plots. These in turn are observed at the reduced linear velocity ν_{opt} (expressed relative to the rate of solute diffusion (D_m) across a particle) that corresponds to the optimal linear velocity μ_{opt}. The columns packed with varying particle sizes yield their lowest h value at reduced velocities ν in the region of 3.4–3.9 (Fig. S1, supporting information). Comparison of the overall column performances is hereafter performed in this narrow range of eluent velocities.

The corresponding optimal linear velocities of the eluent for the three columns are μ_{opt} = 1.65, 3.11 and 4.00 mm/s. The van Deemter plot of the column packed with 1.9 µm DACH-DNB-CSP shows a flat portion at high linear velocities of the eluent, while efficiency degrades appreciably at high flow rates for the 2.6 and 4.3 µm CSPs. Results of the van Deemter analysis are collected in Table 4, that also includes reduced plate height data (h). A speed factor Sf μ_{opt} is also listed for the three columns, where Sf μ_{opt} is taken equal to 1.0 for the reference column packed with the 4.3 µm CSP and for the other columns is taken as the ratio of their optimum flow rates to that of the reference column. Thus, if the columns are operated at their optimum flow rates, the gain in speed of analysis is equal to 1.88 and 2.42 for the 2.6 and 1.9 µm CSPs, respectively.

3.4. Column geometry

In addition to the 100 × 4.1 mm format, we packed a number of columns with differing lengths to study the potentials of our CSPs in both high speed and high resolution modes. We also prepared a

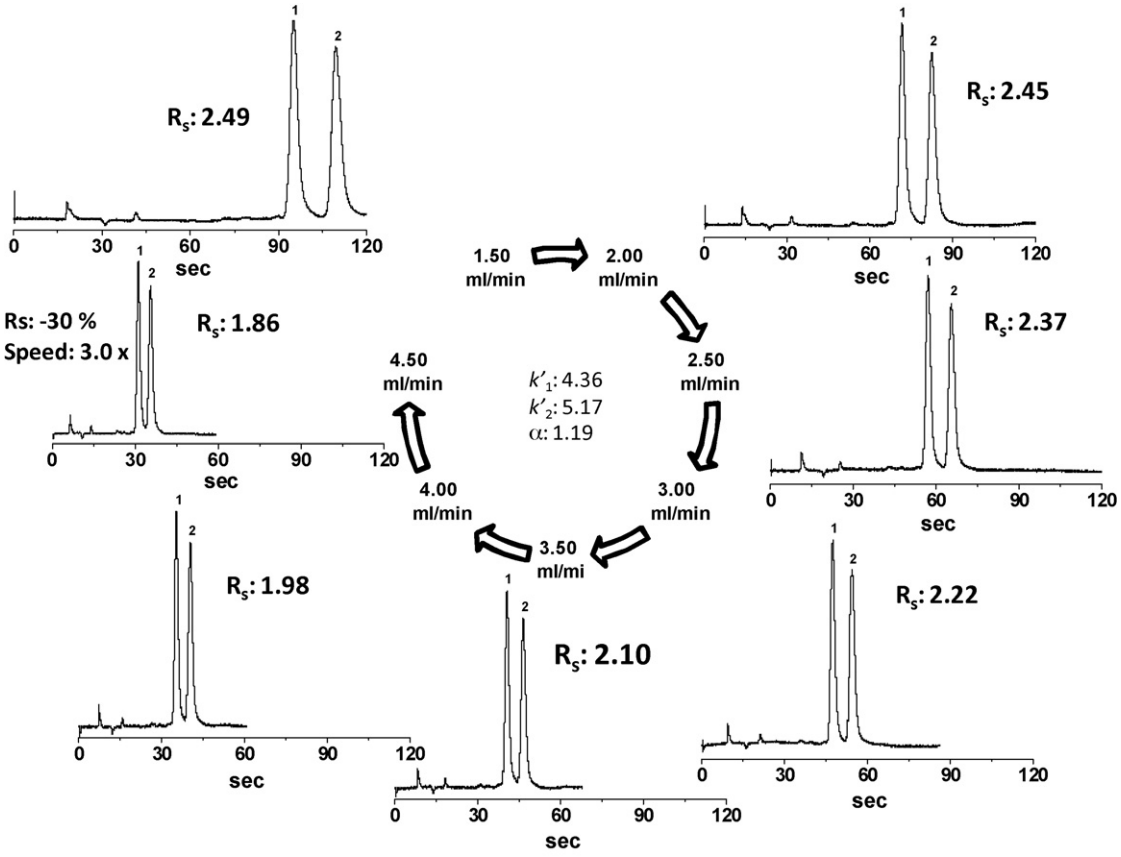

Fig. 7. Very fast resolution of the enantiomers of sulfoxide **1** on the 2.6 μm DACH-DNB CSP packed in a 50 × 4.1 mm column at different flow rates. Experimental conditions as in Table 6.

column with reduced internal diameter (150 × 3.2 mm) to study the impact of this geometric parameter on the overall performances, including eluent consumption. The complete set of columns, their optimal flow rates, and the ratios of column length (L) to particle size (d_p) for each column prepared with the three CSPs are listed in Table 5.

If the column length or the particle size are adjustable parameters, keeping a constant L/d_p ratio will transfer a separation obtained on a long column packed with large particles to a shorter column packed with smaller particles maintaining the same efficiency power in terms of number of theoretical plates [22]. The L/d_p ratio for the columns prepared in this study falls into three intervals (see Tables 2 and 5) spanning the range 19–58 × 10^3, corresponding to column lengths from 50 to 250 mm. As expected, the efficiencies obtained on the columns packed with the smaller sub-2-micron particles are generated at higher optimal flow rates and with elevated column backpressure, compared to the columns having the same L/d_p ratio and packed with larger particles.

The gain in speed that can be achieved using either small particles or short columns, or a combined reduction of both particle size and column length, can be easily calculated from the speed factor due to the shift of the minima in the van Deemter plots with particle size (see before) and from the analysis time reduction due to column shortening. The results for all the combinations of column lengths and particle sizes explored in this study are collected in Table 5. Speed factor changes across the table rows for a given packing are due solely to the column length (Sf_l), whereas speed factor changes across the table columns for a given HPLC column length are due solely to the shift in the minima of the van Deemter curves ($Sf\ \mu_{opt}$). Speed factor changes across diagonals are due to a combination of the two effects ($Sf_l \times Sf\ \mu_{opt}$).

For $L/d_p \times 10^{-3}$ values in the 50–60 range, the separations are accelerated by a factor of 3.2 with the 2.6 μm CSP and by a factor of 6.0 with the 1.9 μm CSP, compared to the reference 4.3 μm CSP.

3.5. Applications to chiral compounds

Enantioselective separations on the three CSPs were studied using a set of chiral compounds (Fig. 4) with sulfur (**1**–**3**), phosphorus (**4**) and carbon stereogenic centers (**5**), together with a stereolabile compound with two stereogenic axes (**6**). Retention factors of the first eluted enantiomers (k_1) and enantioselectivities (α) obtained on the three CSPs are reported in Table 6.

Sulfoxide **1** was used to study the enantioresolution at constant L/d_p ratios, and thus at constant resolution, on the 4.3 μm (150 × 4.1 mm column), 2.6 μm (100 × 4.1 mm column) and 1.9 μm (75 × 4.1 mm column) CSPs (Fig. 5, left side). Retention factors of the enantiomers and enantioselectivity values on the three CSPs are very similar, and the small variations observed between the three columns have little effect on the resolution values that, as anticipated, are close to each other for the three columns. When the separations are operated at the same flow rate of 1.0 ml/min (a value falling between the optimum flow rates for the columns packed with 4.3 and 2.6 μm CSPs) the observed gain in speed by a factor of 1.5 and 2.0 is due solely to the column length reduction. However, separation speed can be increased further by a factor of 2.8_5 and 4.8 if the optimum flow rates are used for the 2.6 and 1.9 μm CSPs, respectively (Fig. 5, right side), leading to very fast separations with unaffected resolution.

Resolution of the enantiomers of sulfoxide **2** (a non-racemic sample) was carried out at varying L/d_p ratios to demonstrate the

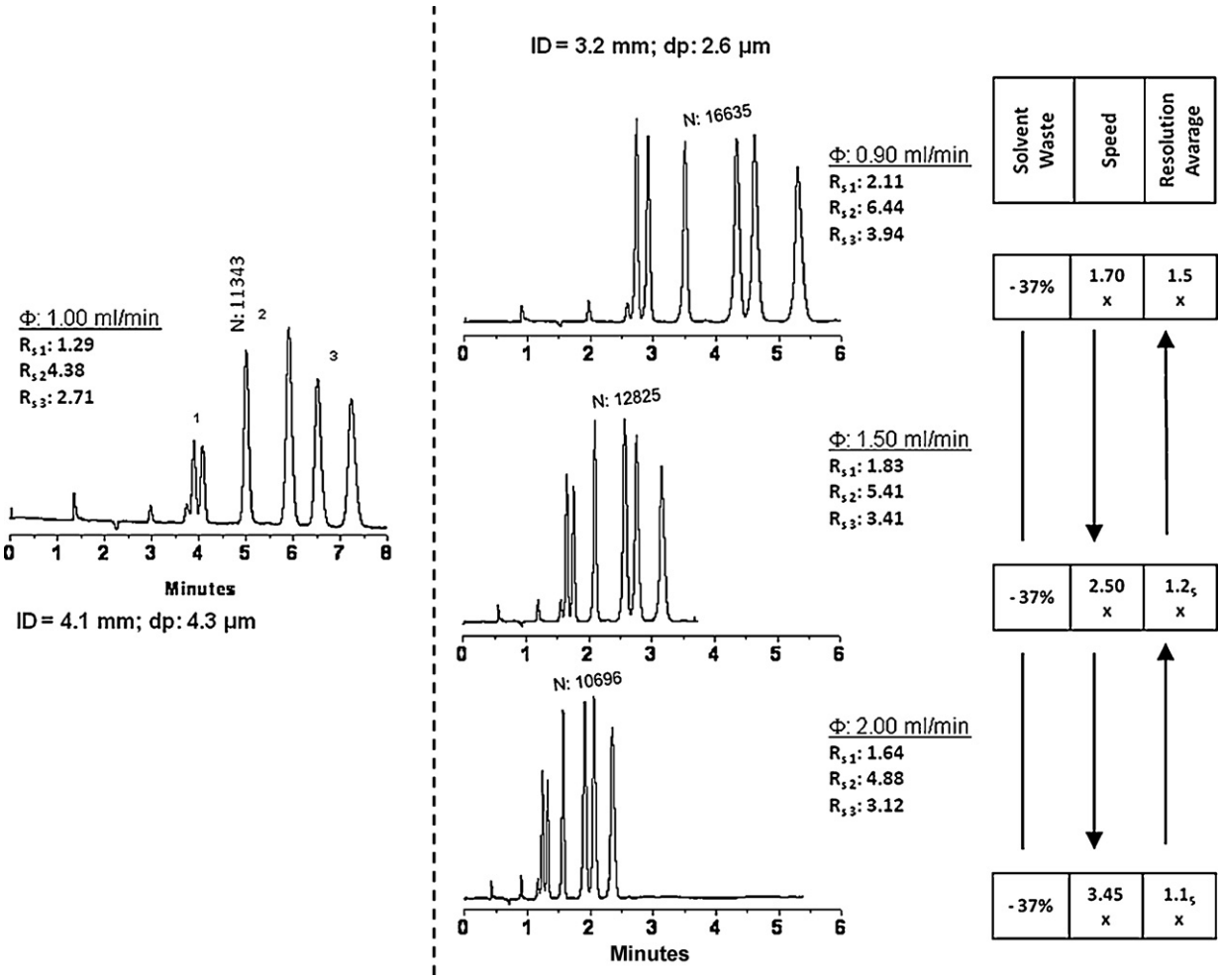

Fig. 8. Resolution of the enantiomers of sulfoxides **1**–**3** on the 4.3 and 2.6 μm DACH-DNB CSPs packed in 150 × 4.1 and 150 × 3.2 mm columns at different flow rates. Experimental conditions as in Table 6.

possibility of transferring a separation on a long column packed with large particles (L = 150 mm, d_p = 4.3 μm; $L/d_p = 35 \times 10^3$; Fig. 6, left) to separations at high speed or at high resolution on a columns packed with smaller particles. Thus, the original resolution value Rs = 4.44 obtained on the reference column operated at a flow rate of 1.00 ml/min is reduced to Rs = 3.81 on a 50 mm column packed with 2.6 μm particles ($L/d_p = 19 \times 10^3$, Fig. 6, right), but the analysis time is cut by one-fifth at a flow rate value of 1.50 ml/min. As the L/d_p ratio is increased to 38×10^3 the resolution returns to the original value but the separation is still faster. With a longer column (L = 150 mm, $L/d_p = 58 \times 10^3$) the resolution increases to Rs = 6.30 and the analysis time is still shorter compared to the reference column. In addition, using the short column packed with 2.6 μm particles (L = 50 mm, $L/d_p = 19 \times 10^3$) leads to a sizeable reduction in the mobile phase consumption and to an increase in sensitivity with UV detection. The increase in sensitivity is an added benefit that can be beneficially exploited in situations where sample amount is limited.

The versatility of the column packed with 2.6 μm particles is evidenced in Fig. 7, where sulfoxide **1** is resolved on the 50 × 4.1 mm column at varying linear velocities of the eluent, ranging from 1.50 ml/min (the optimum value observed on the van Deemter plot) up to 4.50 ml/min. The observed resolutions change from the maximum initial value of 2.49 to the final value of 1.86, with a concomitant threefold gain in speed of analysis and a baseline separation completed in less than 40 s.

A sample containing the sulfoxides **1**–**3** was used to investigate further the effect of changes in the L/d_p ratio and flow rate on the overall resolution in complex mixtures. On the reference 150 × 4.1 mm column packed with the 4.3 μm CSP ($L/d_p = 35 \times 10^3$) the first and second eluted peaks are incompletely separated and the total analysis time is around 8 min, using a flow rate of 1.00 ml/min (Fig. 8, left). Moving to a 150 × 3.2 mm column packed with the 2.6 μm CSP ($L/d_p = 58 \times 10^3$) and delivering the eluent at 0.9 ml/min improves the resolution of the critical pair (1st and 2nd eluted peaks) with a concomitant reduction of the analysis time to less than 6 min. The analysis time can be further reduced to 3.5 and 2.5 min using eluent flow rates of 1.50 and 2.00 ml/min, while keeping a larger resolution of the critical pair compared to the reference column (Fig. 8, right). In this case, the reduction of solvent consumption and the increase in sensitivity are due to the smaller diameter of the column packed with the 2.6 μm CSP.

3.6. Enantioselective UHPLC in the ultra-fast mode

Inspection of the van Deemter plots of our columns (Fig. 3 and Table 4, C term) reveals that 1.9 μm CSP is best suited to very fast applications, in view of the flat portion of the curve observed at high flow rates. Indeed, a short 50 × 4.1 mm column packed with 1.9 μm CSP can separate the enantiomers of several compounds with total analysis time below 1 min. Enantioseparations on the same time

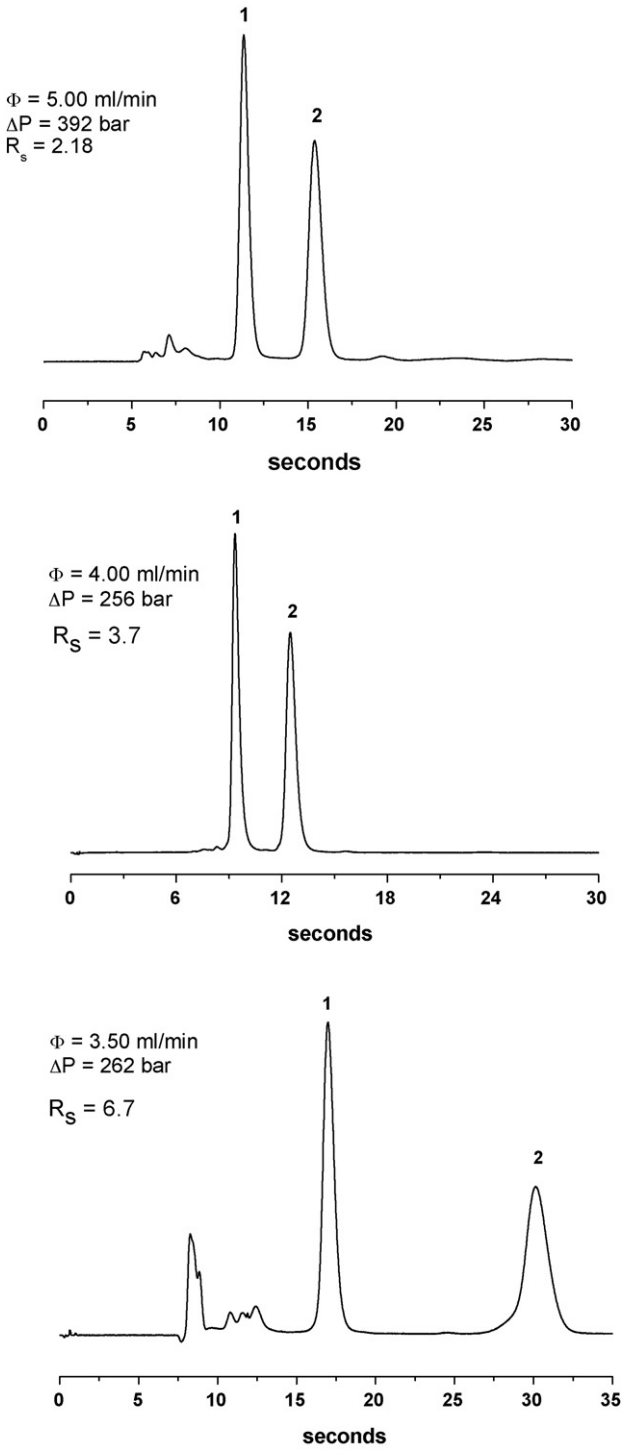

Fig. 9. Ultra-fast resolution of the enantiomers of compounds **2**, **5** and **4**, from top to bottom on the 1.9 μm DACH-DNB CSP packed in a 50 × 4.1 mm column. Flow rates are 5.00 ml/min (top), 4.00 ml/min (middle) and 3.50 ml/min (bottom). Experimental conditions as in Table 6.

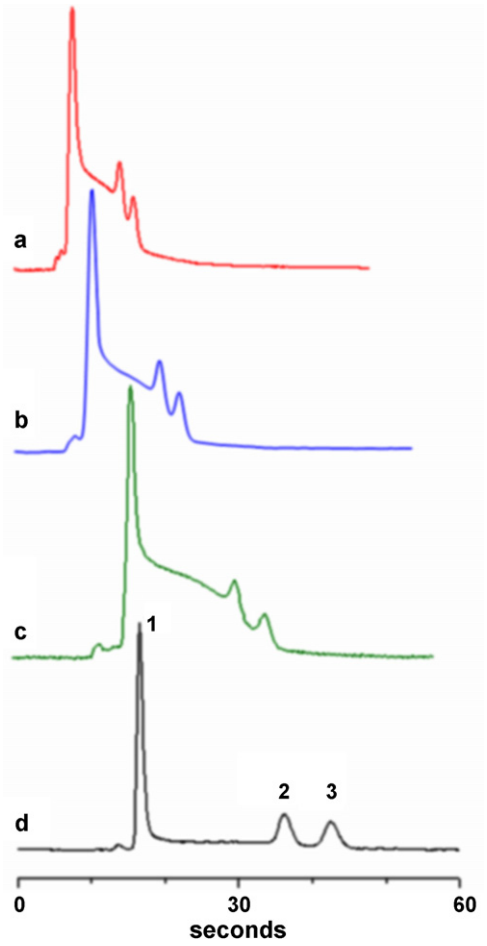

Fig. 10. Dynamic UHPLC of bis-ketone **6** on the 1.9 μm DACH-DNB CSP packed in a 50 × 4.1 mm column. Eluent: hexane/2-propanol/methanol 95/4/1. Column temperature (°C), flow rate (ml/min): (a) 25, 6.00; (b) 25, 5.00; (c) 25, 3.00; (d) 10, 3.00. Numbers on trace (d) indicate achiral (1, meso) and chiral stereoisomers (2 and 3, enantiomers).

scales have been previously reported for 1.5 μm non-porous CSPs [23] and for 3.0 μm polysaccharide CSPs [24]. Examples of such separations are shown in Fig. 9 for compounds **2**, **5** and **4**, from top to bottom. The enantiomers of sulfoxide **2** are separated with an enantioselective value $\alpha = 1.25$, that translates to a resolution value Rs = 2.18 and a total analysis time of 15 s when the eluent is delivered at a flow rate of 5.00 ml/min. The analysis time is even shorter for the naphthamide **5** that is resolved in less than 15 s and with a resolution value Rs = 3.7. Secondary phosphineoxide **4** is resolved at high speed (analysis time less than 35 s) and high resolution (Rs = 6.7) with the eluent delivered at a flow rate of 3.50 ml/min.

3.7. Dynamic e-UHPLC of stereolabile compounds

The chromatographic separation of stereolabile chiral compounds is one particular case in which very fast enantioselective separations find practical applications [25–29]. A dynamic chromatogram, featuring interconverting regions between the resolved peaks, is usually obtained when two or more resolvable stereoisomers interconvert with characteristic rates that fall within the separation time scale. The chromatographic time scale extends from seconds in the cases of very fast e-UHPLC on short columns to several minutes when standard columns are used. For a given column format (column dimensions and particle size of the packing material), typical dynamic plots with peak shape deformations are observed as the column temperature and/or the flow rate of the eluent are changed. Aromatic bis-ketone **6** adopts three different low energy conformations having the carbonyl fragments nearly perpendicular to the naphthyl ring [30]. Two of these conformational isomers, with the carbonyl oxygens pointing on the same side, are chiral and enantiomerically related, whereas the conformation with the carbonyl oxygens pointing on opposite side is achiral. Rotations around the aryl-C=O axes interconvert the three species, whose averaged half life times ($\tau_{1/2}$) at 25 °C are

Table 7
Comparison of column performances on HPLC and UPLC systems using sulfoxide **2** as probe.

Column		UHPLC		HPLC		Loss on Rs (%)
d_p (μm)	$L \times$ I.D. (mm)	N_1[a]	Rs[a]	N_1[a]	Rs[a]	
4.3	150 × 4.1	11,370	4.44	9,700	4.06	−8
	150 × 4.1	16,500	6.30	12,500	5.50	−13
2.6	150 × 3.2	17,000	6.44	11,000	5.00	−22
	50 × 4.1	5,450	3.81	2,800	2.85	−32
1.9	50 × 4.1	6,500	3.98	2,400	2.50	−37

[a] Experimental conditions as in Table 6 for sulfoxide **2**. Averaged retention factor of the first eluted enantiomer $k_1 = 2.7$.

around 30 s. Thus, one expects and finds (Fig. 10) that temperature or analysis time reductions affect the shapes of the dynamic UHPLC plots by changing the interconversion rates (column temperature) or the residence times of the stereoisomers inside the column (flow rate). However, column temperature changes have a more pronounced effect on the final chromatogram (traces c and d) compared to changes in the eluent flow rate (traces a–c): using the 50 × 4.1 mm column packed with 1.9 mm CSP and a column temperature of 10 °C the stereoisomer interconversion during elution is nearly suppressed, and the three peaks are clearly visible and well separated in less than 60 s.

3.8. LC hardware and column performances

A comparison between standard HPLC hardware configuration and UHPLC was carried out using sulfoxide **2** and five different columns packed with the three CSPs (Table 7). The number of theoretical plates for the first eluted peaks (N_1) and the resolution values (Rs) measured using the same column on the two hardware configurations were used to monitor the impact of extracolumn effects on the final performances. Clearly, the loss in resolution observed on the HPLC configuration is only moderate with the 4.3 μm CSP and also with the 2.6 μm CSP packed in the 150 × 4.1 mm column. On the other hand, extracolumn band spreading and resolution losses on the HPLC configuration become substantial with further reduction in the column diameter and/or length, and completely obscure the intrinsic 1.9 μm CSP performances that can be fully exploited on the UHPLC system only.

4. Conclusions

Three brush-type chiral stationary phases based on the known DACH-DNB selector grafted on 4.3, 2.6 and 1.9 micron silica particles have been prepared using an improved, two-step synthetic procedure.

The chiral stationary phases with reduced particle size and packed in short columns provide similar resolutions as those packed in standard column formats, but in considerably shorter times and with the added secondary benefit of solvent saving. Increased throughput and sub-minute enantiomer separations are demonstrated for the shorter columns packed with the 1.9 micron CSP.

Acknowledgement

Financial support from FIRB, Research Program: Ricerca e Sviluppo del Farmaco (CHEMPROFARMA-NET), grant no. RBPR05NWWC_003 is acknowledged.

Appendix A. Supplementary data

Supplementary data associated with this article can be found, in the online version, at doi:10.1016/j.chroma.2009.10.021.

References

[1] C. Welch, Chirality 21 (2009) 114.
[2] S. Allenmark, Chromatographic Enantioseparation, Methods and Applications, Ellis Horwood, New York, 1991.
[3] E. Francotte, W. Lindner (Eds.), Chirality in Drug Research, Wiley-VCH Verlag GmbH & Co. KGaA, Weinhiem, 2006.
[4] G. Subramanian (Ed.), Chiral Separation Techniques—A Practical Approach, 3rd ed., Wiley-VCH, Weinheim, 2007.
[5] J.C. Giddings, Anal. Chem. 37 (1965) 60.
[6] J.H. Knox, J. Chromatogr. Sci. 15 (1977) 352.
[7] H. Poppe, J. Chromatogr. A 778 (1997) 3.
[8] N. Wu, J.A. Lippert, M.L. Lee, J. Chromatogr. A 911 (2001) 1.
[9] A.D. Jerkovich, J.S. Mellors, J.W. Jorgenson, LC–GC Eur. 16 (2003) 20.
[10] R.E. Majors, LC–GC N. Am. 23 (2005) 1248.
[11] R.E. Majors, LC–GC N. Am. 24 (2006) 248.
[12] G. Desmet, P. Gzil, D.T.-T. Nguyen, D. Guillarme, S. Rudaz, J.-L. Veuthey, N. Vervoort, G. Torok, D. Cabooter, D. Clicq, Anal. Chem. 78 (2006) 2150.
[13] D. Guillarme, D.T.-T. Nguyen, S. Rudaz, J.-L. Veuthey, J. Chromatogr. A 1149 (2007) 20.
[14] P.W. Carr, X. Wang, D.R. Stoll, Anal. Chem. 81 (2009) 5342.
[15] G. Guiochon, J. Chromatogr. A 1126 (2006) 6.
[16] F. Gasparrini, F. La Torre, D. Misiti, C. Villani, J. Chromatogr. 539 (1991) 25.
[17] F. Gasparrini, D. Misiti, C. Villani, Chirality 4 (1992) 447.
[18] F. Gasparrini, D. Misiti, C. Villani, J. Chromatogr. A 906 (2001) 35.
[19] G. Cancelliere, I. D'Acquarica, F. Gasparrini, M. Maggini, D. Misiti, C. Villani, J. Sep. Sci. 29 (2006) 770.
[20] I.-C. Wei, R.L. Rowley, J. Chem. Eng. Data 29 (1984) 332.
[21] I. Halàsz, H. Schmidt, P. Vogtel, J. Chromatogr. 126 (1976) 19.
[22] K.J. Fountain, U.D. Neue, E.S. Grumbach, D.M. Diehl, J. Chromatogr. A 1216 (2009) 5979.
[23] T. Welsch, C. Schmidtkunz, B. Müller, F. Meier, M. Chlup, A. Köhne, M. Lämmerhofer, W. Lindner, Anal. Bioanal. Chem. 338 (2007) 1717.
[24] T. Zhang, P. Franco, LC–GC Eur. 21 (2008) 430.
[25] O. Trapp, V. Schurig, J. Amer. Chem. Soc. 122 (2000) 1424.
[26] F. Gasparrini, I. D'Acquarica, M. Pierini, C. Villani, J. Sep. Sci. 24 (2001) 941.
[27] I. D'Acquarica, F. Gasparrini, M. Pierini, C. Villani, G. Zappia, J. Sep. Sci. 29 (2006) 1508.
[28] C. Villani, F. Gasparrini, M. Pierini, S. Levi Mortera, I. D'Acquarica, A. Ciogli, G. Zappia, Chirality 21 (2009) 97.
[29] C. Wolf, Chem. Soc. Rev. 34 (2005) 595.
[30] D. Casarini, L. Lunazzi, F. Pasquali, F. Gasparrini, C. Villani, J. Am. Chem. Soc. 114 (1992) 6521.